Effect of Injection Angle in Mixing and Combustion Characteristics of Scramjet Combustor

MSR Chandra Murty and Debasis Chakraborty
Directorate of Computational Dynamics, Defence Research and Development Laboratory
Hyderabad – 500058, India. Tel: +91-40-24583310, Fax: +91-40-24340037
E-mail. debasis_cfd@drdl.drdo.in

Abstract
Effect of injection angle in mixing and combustion in a scramjet combustor is numerically simulated. Three dimensional Navier Stokes equations alongwith k–ε turbulence model are solved using commercial CFD software. Both infinitely fast rate kinetics and single step finite rate kinetics are used to model chemical kinetics. Turbulence chemistry interaction is modeled by Eddy Dissipation Concept (EDC). Good agreement between the Computed and experimental results for angular Injection (30°) and perpendicular injection forms the basis of further analysis. More flow blockage has caused significant upstream interaction for perpendicular injection and terminal shock is seen to anchor upstream of combustor step; while for angular injection, the flow field is predominantly supersonic. Single step finite rate chemistry show comparatively low pressure and lesser upstream interaction because of the presence of backward reaction. Thermochemical variables are anlysed to study the effect of angle of injection on nature of combustion (whether premixed or diffusive), heat release pattern, combustion efficiency etc.

Keywords: Scramjet, CFD, Turbulence-chemistry interaction

1. INTRODUCTION

Greater understanding of mixing and combustion process in supersonic flow is necessary to develop efficient scramjet engine for hypersonic air breathing vehicles. The flowfield inside the combustor is very complex where fluid dynamics and chemistry interact very strongly. Starting from pioneering work of Ferri [1], supersonic reactive flows are explored enormously over 50 years in different countries focusing on different aspects of, fuel injection, ignition, flame holding, engine performance, intake combustor interaction etc. Several analytical, experimental, computational studies are still being carried out to understand complex mixing and combustion process inside the scramjet combustor.

With the advent of powerful computers and robust numerical algorithms, CFD complements difficult-to-perform experiments and thus plays a major role in developing a comprehensive understanding of the key phenomena that dominate performances. To accurately model a scramjet flowfield, CFD must adequately resolve several complex physical processes, including three-dimensionality, shock–boundary layer interaction, turbulent mixing of high-speed streams, and combustion of fuel. Because of the limitation of current turbulence models, it is very difficult to predict apriori all the finer flow details for complex shock – boundary layer interaction and flow separation. The existing combustion models are mostly developed for low speed flows and the development of combustion model for high speed flows is in a formative stage. Although it is reported in the literature [2–4] that for mixing limited flows, Eddy Dissipation Concept (EDC) based combustion models can predict the overall features of mixing and combustion in high speed turbulent reacting flows, the validation of combustion models against reliable experimental data may remain a continuous process. The validation exercise will also help to estimate the range of application and error band of CFD tools before they are used in design exercise.

Recently, to validate CFD data, a scramjet model known as SCHOLAR has been tested at NASA Langley's Direct Connect Supersonic Test facilities [5–8]. Hydrogen fuel is injected to Mach 2 airstreams with 1200 K temperature in a divergent duct. Apart from surface pressures, cross sectional distribution of temperature and species mass fractions are measured at various cross sections using CARS thermometer. The other notable features of the experiments are: (1) flow field contains some relevant features of high-speed engine flow path such as supersonic mixing and combustion with embedded regions of subsonic and recirculating flow (2) geometry is simple so proper interpretation of data is possible (3) experiments have well defined and well controlled inflow and boundary conditions and well quantified uncertainties. Two experiments with two different injection patterns namely, 30° angular injection and perpendicular injection were conducted to find out the effect of injection angle in the mixing and combustion process in the scramjet combustor flow field. Various numerical simulations were performed in the literature for both angular injection [8–13] and perpendicular injection [12–13] cases using RANS [8–13] and LES [14–15] methods with advanced models of turbulence transport and detailed chemical kinetics. DES [16] and LES [17] simulations were also presented for perpendicular injection cases. It has been observed that with the addition of turbulence-chemistry interaction, there is a dramatic increase in the turbulent diffusivity throughout the flame region. It is clear that modeling issues in high speed turbulent reactive flows need further investigation since these turbulence and chemical reaction models are computationally prohibitive for practical engineering applications. Recently, Murthy and Chakarborty [18] have demonstrated that standard engineering tools (simple chemical kinetic scheme and simple turbulence-chemistry interaction model) can predict overall features of the mixing and reaction of scholar experiment for angular injection case.

The present study explores numerically the experimental condition of perpendicular injection case of SCHOLAR experiment and compares the computed results with the experimental values. Computed thermochemical variables for perpendicular and angular injection are also compared to address various modeling issues and to have a better insight of mixing and combustion processes occurring inside the scramjet combustor.

2. DESCRIPTION OF TEST SET UP AND THE COMBUSTOR FOR WHICH THE SIMULATION IS CARRIED OUT

The SCHOLAR experiment [3–8] has been discussed extensively in the literature. The schematic of experimental conditions for both angular and perpendicular injection cases are shown in Fig. 1. Vitiated air corresponding to Mach 7 enthalpy is produced in a heater by combustion of Hydrogen with premixed oxygen and air. Oxygen is replenished so that the vitiated air at combustor entry will have

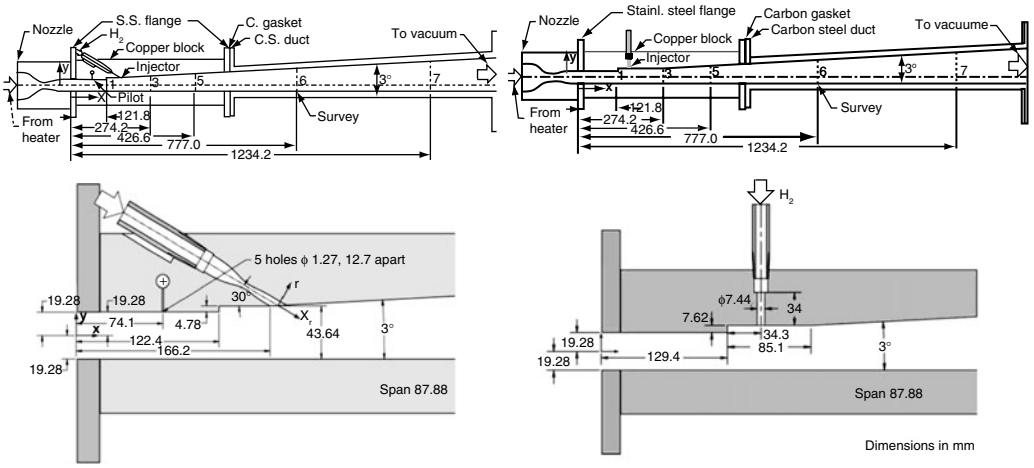

Figure 1. Schematic of Scholar experiment Combustor and Exploded view near angular fuel injector for (a) angular injection (b) perpendicular injection.

Table 1. Inflow parameters at combustor entry and fuel injector exit

	Angular injection		Vertical injection	
Parameters	**Vitiated air**	**Injector**	**Vitiated air**	**Injector**
Total pressure (MPa)	0.765 ± 0.008	3.44 ± 0.07	0.795 ± 0.015	1.35 ± 0.025
Total temp (K)	1827 ± 75	302 ± 4	1490 ± 75	290 ± 5
Mach No.	1.989 ± 0.005	2.5	2.007 ± 0.005	1.0
Mass flow rate Kg/sec	1.2434 ± 0.0136	0.04576	1.4731 ± 0.0096	0.03533
X_{H_2}	0.0000	1.0	0.003	1.0
X_{O_2}	0.2321	0	0.227	0
X_{H_2O}	0.2041	0	0.176	0
X_{N_2}	0.5638	0	0.594	0

oxygen mass fraction as that of pure air. The layout and dimension of the combustor model is shown in Fig 1. The combustor duct consists of two constant area isolators that end in a step in the top wall. Downstream of the step there is another short constant area section followed by 3° divergence on the top wall upto the exit of the combustor. The length of the combustor is 1.45 m and the width (0.88 m) is constant throughout the combustor. The height of the combustor at entry is 38.86 mm while the height at the exit is 112 mm. There are marginal differences in the geometries near the injector locations. The step height and the length of the constant area duct before the injector for the perpendicular injector geometry is higher by 3 mm and 7 mm respectively.

The heater stagnation pressure, stagnation temperature and mass flow rates and equivalence ratio for the two geometries are compared in Table 1. The difference in the inflow properties of heater and injector is due to the fact that the angular injection test case was carried out are for Mach 7 total flight enthalpy condition whereas the perpendicular injection test case corresponds to Mach 6 flight enthalpy condition. The high-pressure vitiated air is accelerated through a water-cooled Mach 2 nozzle before it enters the combustor entry test section. All the uncertainties are due to mass flow rate measurement error and run-to-run variation in heater condition. Wall pressures are measured at the top, bottom and side walls. To enable the measurement of temperature field by CARS (Coherent Anti-Stokes Raman Spectroscopy) beam, few transverse slots are provided in the combustor (mark 1, 3, 5, 6, 7) at a distance of 121.8, 274.2, 426.6, 777.0, 1234.2 mm from the combustor entry.

3. COMPUTATIONAL METHODOLOGY

Simulations are carried out using a commercial CFD software Fluent [19]. It solves three-dimensional Navier Stokes Equation in a structured, multiblock grid system using a collocated variable arrangement. To simulate high Mach number compressible flow (as in the present case), density based solver is used alongwith Roe Flux Difference Splitting Scheme [20] for spatial discretization and 1st order implicit Euler Scheme for temporal discretization. Wilcox's $k-\omega$ model is used to model turbulence.

The chemistry of Hydrogen-air combustion reaction is represented on a molar basis by $H_2 + 0.5O_2 = H_2O$. The mixing rate determined from the Eddy Dissipation Model (EDM) is given as.

$$R_{k,edm} = - A_{ebu}\rho\frac{\varepsilon}{K}\min\left\{Y_f, \frac{Y_o}{r_k}, B_{ebu}\frac{Y_p}{1+r_k}\right\}$$

where ρ, Y_f, Y_o and Y_p are the density and mass fractions of fuel, oxidizer and products respectively, A_{ebu} and B_{ebu} are the model constants and r_k is the stoichiometric ratio.

In the single step finite rate chemistry the following reversible reacting involving H_2, O_2 and H_2O is considered.

$$H_2 + O_2 \Leftrightarrow H_2O$$

With pre-exponential factor (A) of 1.02×10^{19}, power constant (N) of 0 and activation temperature (E/R) of 8052.

Following Magnussen and Gran [21–23], the mean reaction rate for the species i (w_i) is given by H

$$\frac{\bar{\dot{w}}_i}{\rho} = \frac{\gamma^2 \chi}{\tau^*}(Y_i^0 - Y_i^*)$$

Where χ is the fraction of the fine structures where reaction occurs and superscripts '0' and '*' refers to the surrounding fluids and fine structure region. τ^* is the time scale for the mass transfer between the fine structures and the surroundings. The fine structure is considered as a constant pressure homogeneous reactor where all the properties are time dependent and no spatial gradient exists. A more detailed description of the EDC based finite rate combustion model is available in Ref. 23.

Finite rate calculations are performed with the help of Chemkin software. A coupling code is written to make calls between Chemkin and Fluent. At every time step δt, the current solution field are taken from Fluent solver including mass fraction of every species, temperature and pressure. These values are used as initial conditions for Chemkin solver. Chemkin solves the reaction rates for each species and estimates the mass fractions of all species and temperature. These values will be transferred to Fluent solver. This process continues for every iteration of Fluent solver.

4. RESULTS AND DISCUSSION

The computational domain of the total set up is divided into two parts namely (1) facility nozzle and (2) combustor with fuel injection system. These flow fields are simulated sequentially and the solution at the exit plane of the facility nozzle provides values of various flow variables at combustor entry plane. Taking advantage of the geometrical symmetry only half width of the combustor is simulated. In the simulation, x-axis is taken along width of the combustor, while y and z axes are along the height and length of the combustor respectively. The origin is placed at combustor inflow center. Injector geometry is simulated and appropriate hexahedral grid is taken in the injector region. Multiblock structured grid of size 38*60*553 is employed in the simulation. The grid distribution in the computational domain is shown in Fig. 2. The grid independence of the solution is achieved and uncertainties of numerical errors are quantified through Grid – Convergence Index (GCI).

Stagnation pressure of 0.79 MPa and stagnation temperature of 1490 K are specified at the inflow plane of convergent section of the facility nozzle. The injector provides transverse sonic H_2 to the combustor chamber. Inflow condition at the inlet of the hydrogen injector is assumed subsonic and the stagnation pressure of 1.35 MPa and stagnation temperature of 290 K is specified at the inflow plane of the injector. Supersonic outflow conditions are specified at the outflow boundary.

For perpendicular injection case, four different simulations were carried out including no injection, injection without reaction (mixing), reaction with infinitely first rate (FC) kinetics and and reaction with single step finite rate chemistry (SSC). The Mach number distributions in all these four cases are shown in Fig. 3. For no injection case (case-a), the repeated reflections of expansion waves from the step upstream of the injection point are clearly visible. The injection caused the blockage of incoming supersonic flow and an oblique shock is seen near the injection region (case-b) and the flow downstream of the reaction remains supersonic. For the reacting cases (case c & d), heat release due to reaction decelerated the flow to subsonic value and the upstream effect is felt upstream of the injector. The upstream effect is clearly seen in the comparison of axial distribution of top surface pressure of the combustor presented in Fig. 4. The injection of fuel has increased the local pressure near the

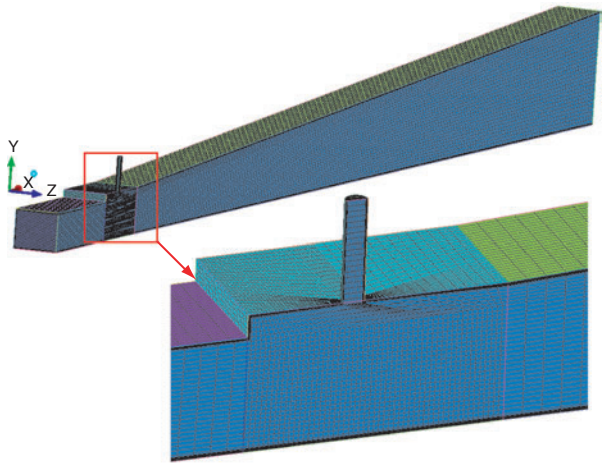

Figure 2. Grid distribution for perpendicular injection case.

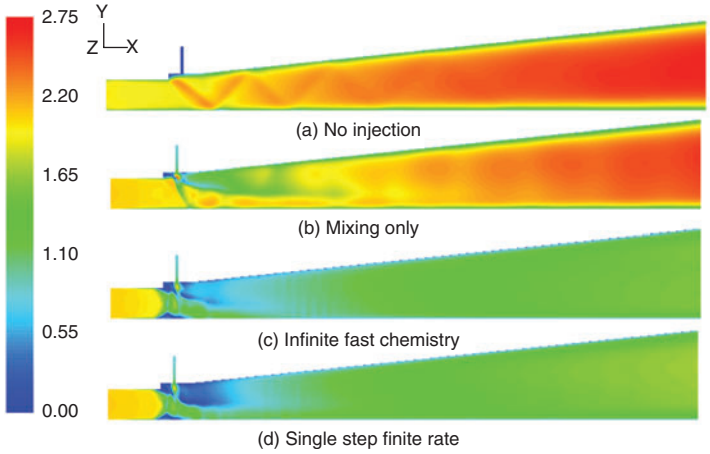

Figure 3. Mach number distribution at the plane of symmetry (a) no injection (b) injection without reaction (mixing) (c) FC calculation (d) SSC calculation.

injector but the reaction has increased the surface pressure considerably. The difference between the reacting and nonreacting pressure is responsible for the thrust produced in the combustor. Terminal shock is seen positioned ahead of the injector because of heat release caused due to reaction. Since the heat release in Fast Chemistry (FC) is much more compared to SSC, terminal shock is moved further upstream in the combustor. The surface pressure distributions at the top, bottom and side walls are compared in Fig. 5 which indicates that three dimensionality effect in the flow field is confined near the injector.

The Mach number distributions at the plane of injection for both angular and perpendicular injection cases are compared in Figure 6 for SSC calculation. It is very clear from the figure that for perpendicular injection, significant amount of upstream interaction with normal shock anchored at 120.3 mm upstream of the injector for the perpendicular injection case and the flow field is predominantly subsonic near the injection zone. On the other hand, predominant supersonic flow prevails for the angular injection case. It is to be noted that that equivalence ratio of the perpendicular injection case is 0.7 compared to 1.0 for the angular injection case. More flow blockage and intense reaction due to low speed near the injector is responsible for the upstream interaction.

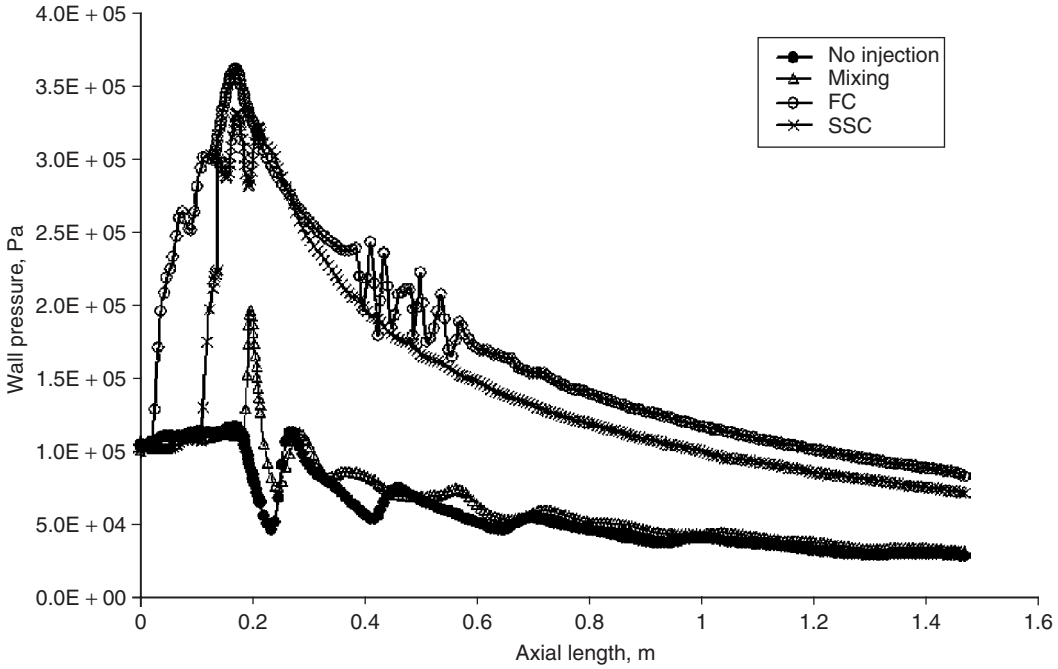

Figure 4. Surface pressure comparison for the cases a) No injection b) Mixing c) FC and d) SSC.

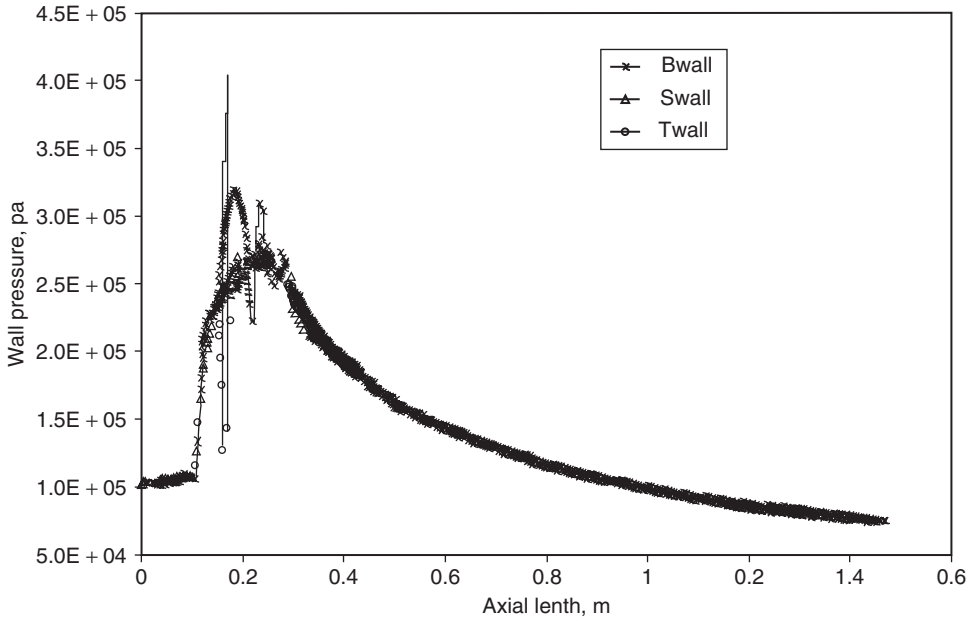

Figure 5. Axial distribution of wall pressure for bottom, side and top walls (SSC).

The water mass fraction distributions at the injection plane presented in Figure 7 describe the differences in reaction pattern between the two cases. Fuel has penetrated much downstream for angular injection case, compared to the perpendicular injection case. Higher temperature and lower velocity for the perpendicular injection case is responsible for more reaction near the injector.

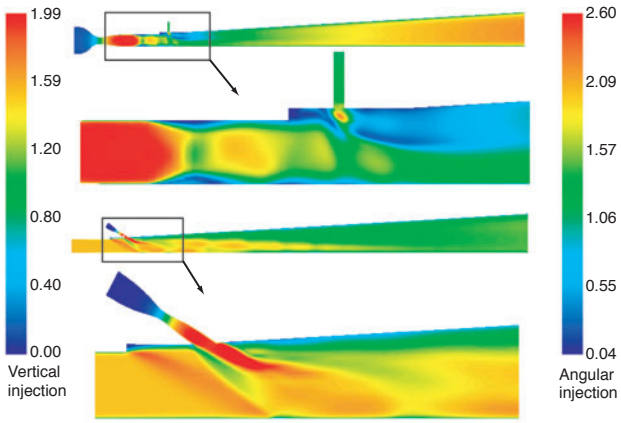

Figure 6. Comparison of Mach number in symmetry plane for a) Vertical injection b) Angular injection.

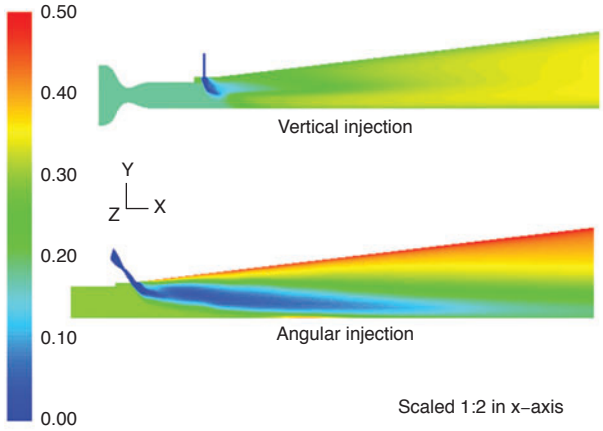

Figure 7. Comparison of H_2O mole fraction in symmetry plane for a) Vertical injection b) Angular injection.

Computed surface pressure for the perpendicular injection case for two different chemical kinetics namely FC and SSC are compared with experimental results in Figure 8. The Experimental result for the nonreacting case and SSC computation for the angular injection case are also included in the figure for comparison. In the divergent portion of the combustor, where the majority of thrust is produced, the computed surface pressure matches well with the experimental values. Both FC and SSC calculation show higher pressure near the injector compared to the experimental values. Instantaneous heat release due to faster chemistry employed in the calculation is conjectures to be the cause of higher surface pressure. Since SSC is comparatively slower than FC, both the pressure peak and the upstream interaction are lower for SSC compared to the FC. A more detailed H_2 – air chemistry is required for better match with the experimental results.

Computed Oxygen mole fraction distribution at various axial stations for the angular and perpendicular injection cases are compared with experimental results in Figure 9. Although qualitative features of experimental) 2 mole fraction distribution have been captured in the numerical simulations, finer details of the reacting flow field differ between the experiment and computation. Diffusion is seen to be more in the experimental condition compared to the numerical calculation. Whether calculation with varying turbulent Schmidth number can resolve this difference is not known. Comparison of

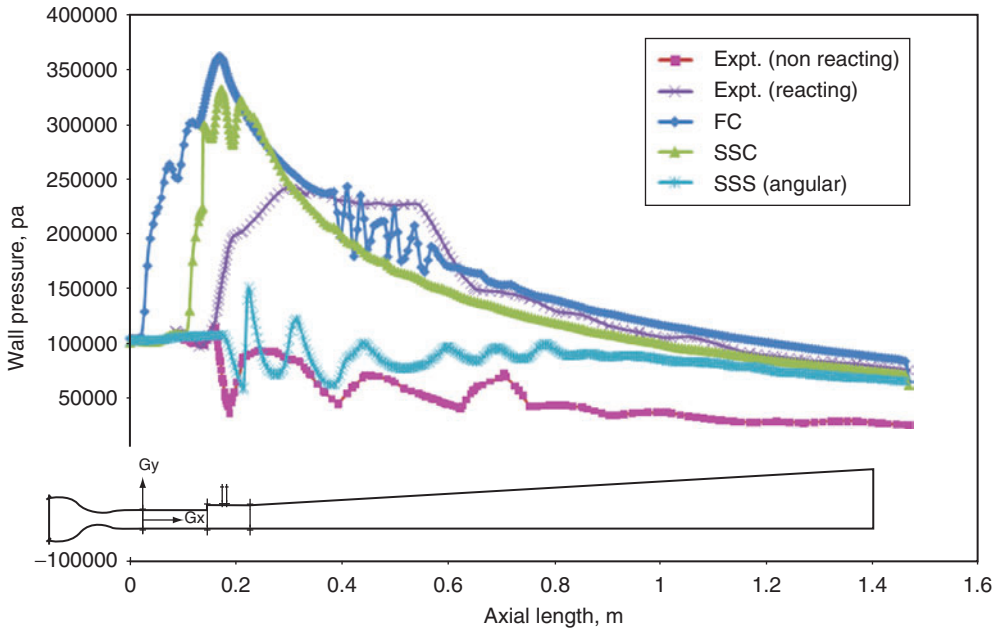

Figure 8. Axial distribution of top surface pressure distribution.

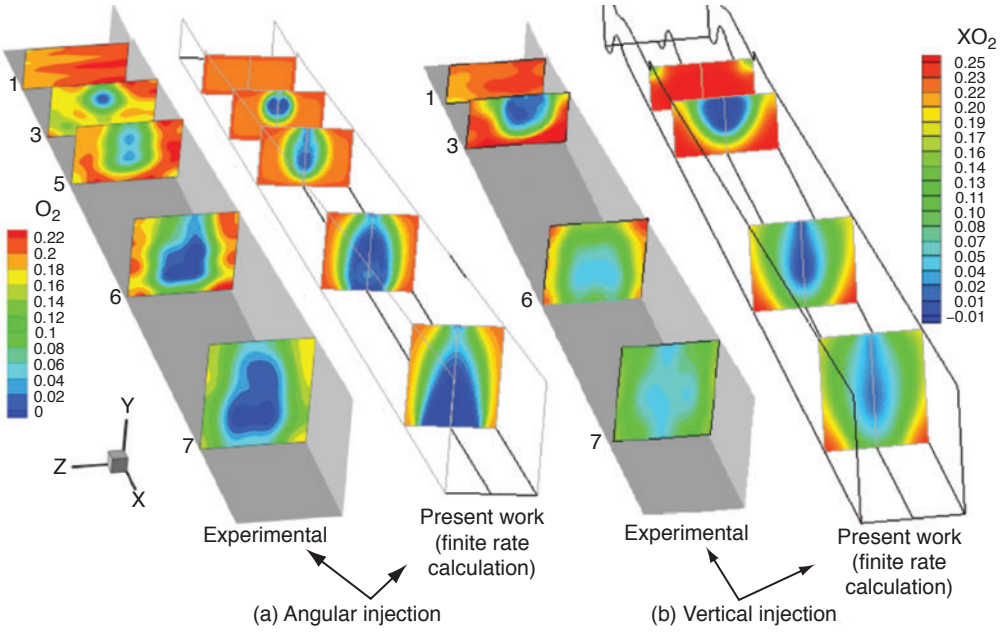

Figure 9. O_2 mole fraction distribution at various axial stations (a) angular (experimental and SSC) (b) perpendicular (experimental and SSC).

experimental and numerical distribution of H_2 Mole fraction, N_2 Mole fraction and temperature at different cross sections are shown in Figs 10–12. Although a good qualitative match is obtained between the two, finer details differ significantly between the two.

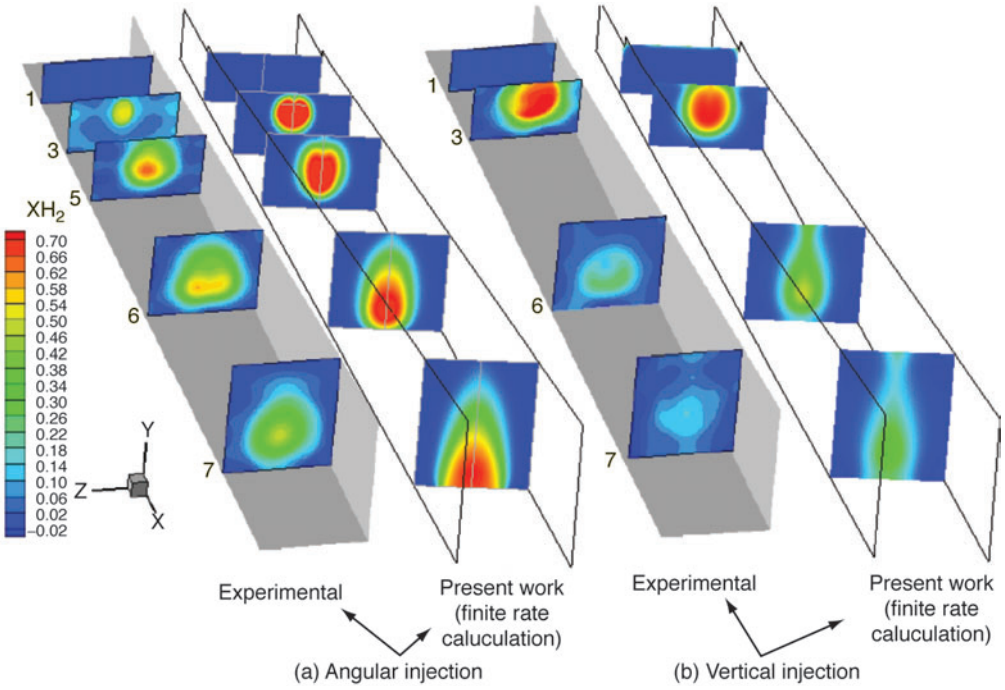

Figure 10. H_2 mole fraction distribution at various axial stations (a) angular (experimental and SSC) (b) perpendicular (experimental and SSC).

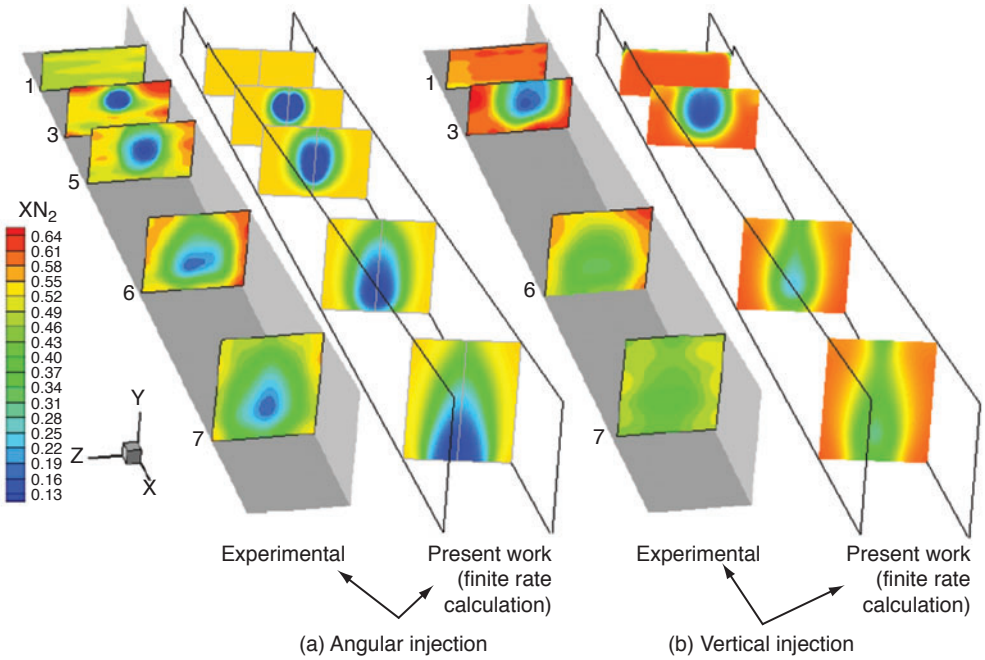

Figure 11. N_2 mole fraction distribution at various axial stations (a) angular (experimental and SSC) (b) perpendicular (experimental and SSC).

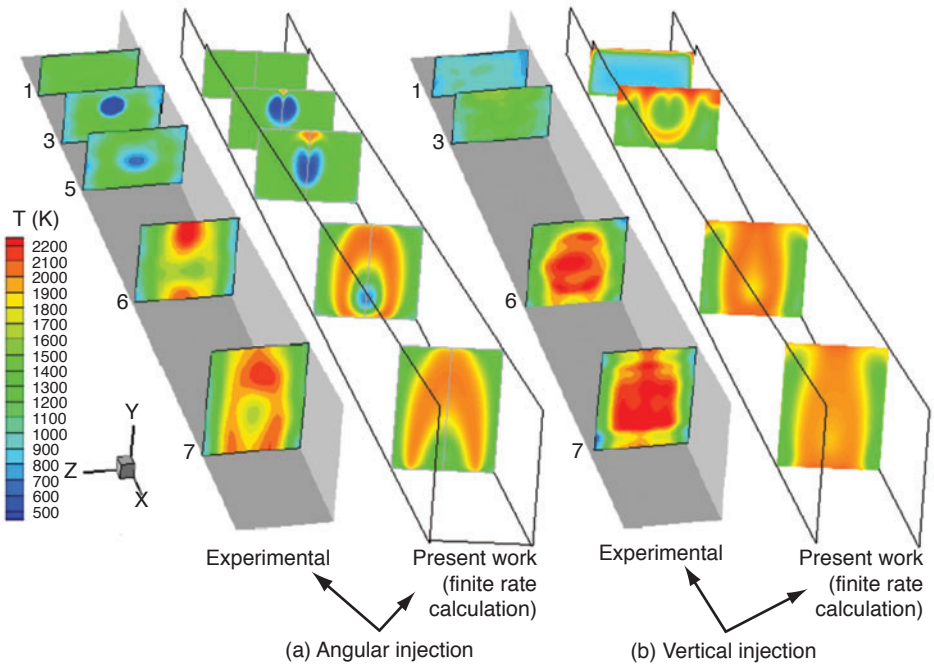

Figure 12. Static Temperature (K) distribution at various axial stations (a) angular (experimental and SSC) (b) perpendicular (experimental and SSC).

To find out the region of premixed and diffusion dominated combustion, the distribution of the term $\nabla Y_{H_2} \bullet \nabla Y_{O_2}$ in the symmetry plane is compared between the angular and perpendicular injection in Fig. 13. Yamashita et al [24] used this index to determine the zone of premixed and diffusion combustion in the mixing layer. The basic idea is that if the dot product of the gradient of fuel and oxidizer mass fraction is strongly negative, then the zone is dominated by diffusive combustion since the flame is fed by the oxidizer and fuel from opposite direction; if the quantity is strongly positive, the zone is affected by premixed combustion since the fuel and oxidizer is fed from the same side. From the figure it is clear that for angular injection case, the burning near the injection is mostly diffusive in nature and small region of premixed combustion is seen in the upper portion of the

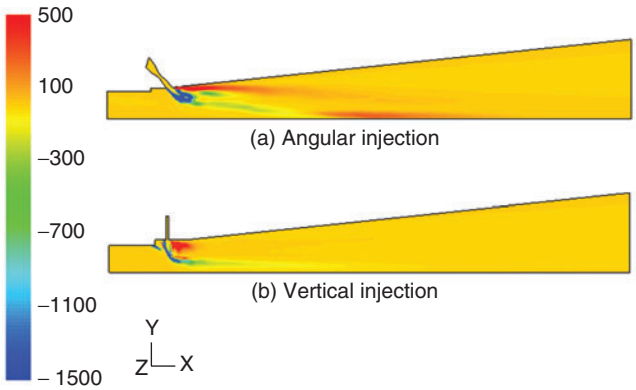

Figure 13. Distribution of $\nabla Y_{H_2} \bullet \nabla Y_{O_2}$ at injection region for a) angular injection b) vertical injection.

combustor. For perpendicular injection, diffusive combustion is very much limited and the reaction is mostly premixed.

The velocity, temperature and water mass fraction profile in the symmetry plane at x = 1234 mm (station 7) is compared between the angular injection and perpendicular in jection in Fig. 14. We can observe that velocity profile for angular and perpendicular injection case is similar in nature, but the temperature and mass water mass fraction profiles varies significantly. It is seen that while velocity changes are effected by gas dynamics while the change in the temperature and water mass fraction is related to the chemical reactions.

The axial distribution of combustion efficiency for equivalence ratio of 1.0 is presented in Fig. 15. Following Kim et al [25], combustion efficiency is defined as

$$\eta_c(x) = 1 - \frac{\int \rho u y_F dA}{(\rho u y_F dA)_{x=0}}$$

y_F is the mass fraction of hydrogen fuel. Although the axial distribution of combustion efficiency for both the injection pattern show the similar value (~ 95%) at the combustor exit, perpendicular injection show faster reaction compared to the angular injection.

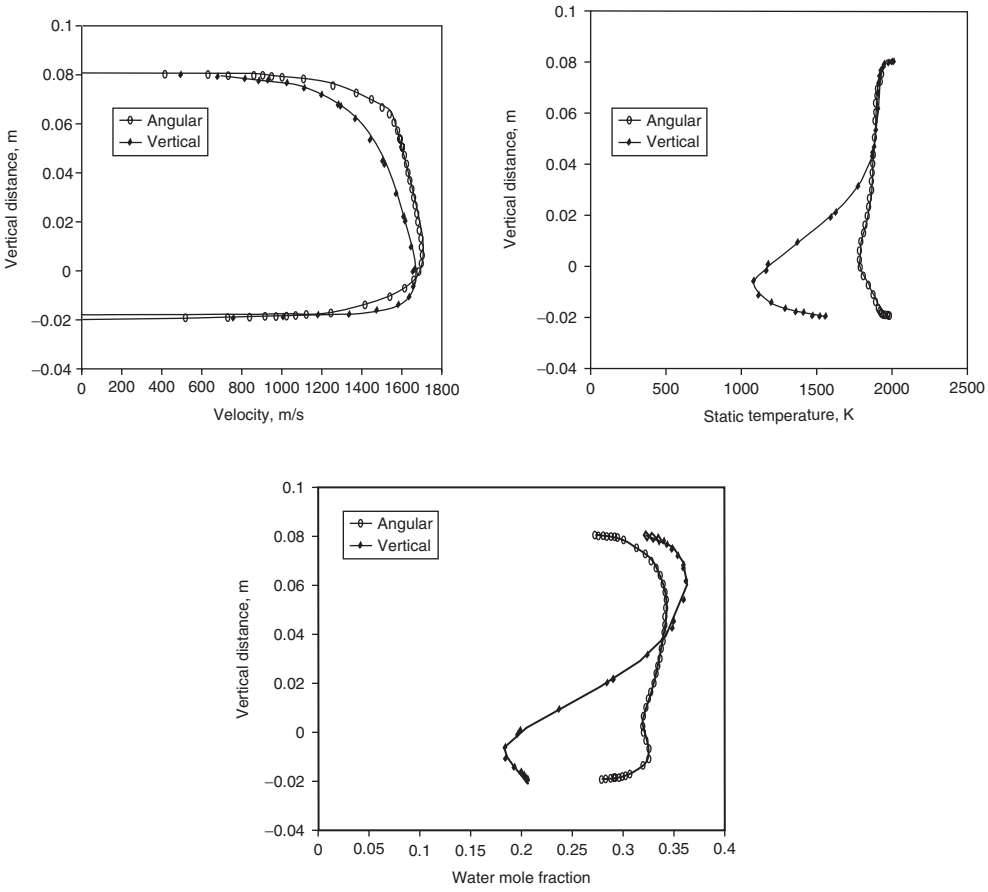

Figure 14. Profiles of thermochemical variables at X = 1234.2 (Plane-7) (a) Velocity (m/sec) (b) Static temperature (K) and (c) Water mole fraction.

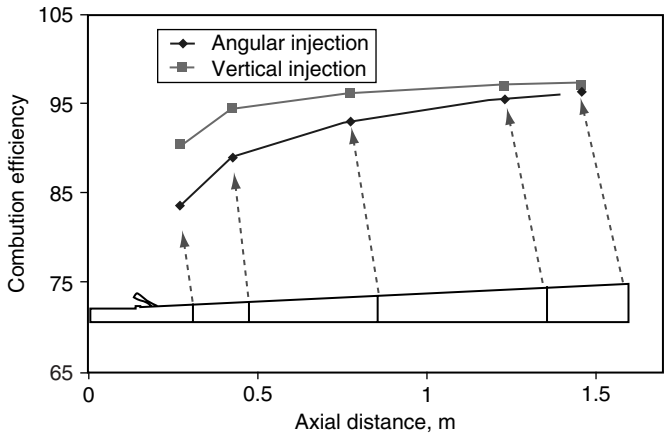

Figure 15. Axial distribution of combustion efficiency.

5. CONCLUSIONS

The effect of injection angle on mixing and combustion behavior in Hydrogen based scramjet combustor is studied. Thermochemical variables for perpendicular injection case are compared with that of angular injection case. More flow blockage and intense reaction caused significant upstream interaction for the perpendicular injection case. Because of higher temperature and low velocity, reactions are more intense for the perpendicular injection case compared to angular injection case. Although, in the divergent portion of the combustor, the computed pressure matches well with experimental value, predicted surface pressures with Fast chemistry show higher value near the injector and more upstream interaction because of instantaneous heat release assumption. Single step finite rate chemistry show comparatively low pressure and lesser upstream interaction because of the presence of backward reaction. A more detailed H_2 –air chemistry is required for capturing the flow feature near the injector. Angular injection shows that the burning near the injection is mostly diffusive and small region of premixed combustion is present in the upper part of the combustor; while diffusive combustion is very much limited and the reaction is mostly premixed for perpendicular injection. It is also observed that injection pattern does not change the velocity profile at down stream regions; but significantly alters the reaction and heat release pattern. The axial distribution of combustion efficiency shows that the reaction is nearly complete at the exit section for both the injection case.

REFERENCES

[1] A Ferri: "Review of problems in application of Supersonic Combustion" Journal of the Royal Aeronautical Society, Vol 68, No. 645, pp 575–597, 1964.

[2] Debasis Chakraborty, P. J. Paul and H. S. Mukunda: "Evaluation of Empirical Combustion Models for High Speed H_2/air Confined Mixing Layer Using DNS Data", *Combustion and Flame*, Vol 121, pp 195–209, April, 2000.

[3] P. Manna, Ramesh Behera and Debasis Chakraborty: "Thermochemical exploration of a cavity based supersonic combustor with liquid kerosene fuel" *Journal of "Aerospace Sciences and Technologies"* Vol 59, No 4 pp 246–258, Nov, 2007.

[4] Debasis Chakraborty (2010) "CFD based design of kerosene fueled scramjet combustor", International Journal of Hypersonics, Vol 1, No 1, pp 14–29

[5] Cutler, A.D., Danehy, P.M., Springer, R.R., DeLoach, R., and Capriotti, D.P., "CARS Thermometry in a Supersonic Combustor for CFD Code Validation", AIAA Paper 2002-0743, 2002.

[6] A.D. Cutler, P.M. Danehy, S.O'Byrne, C.G. Rodrigues and J.P. Drummond: "Supersonic Combustion Experiment for CFD Model Development and validation", AIAA Paper No. 2004-266.

[7] Tedder, S.A., Byme, S.O., Danehy, P.M. Cutler, A.D. "CARS Temperature and species concentration measurements in a supersonic combustor with normal injection", AIAA Paper 2005.

[8] C.G. Rodrigues and A.D. Cutler: "Computational Simulation of a supersonic-Combustion Benchmark Experiment" AIAA 2005-4424.

[9] A.D. Cutler, P.M. Danehy, S.O'Byrne, C.G. Rodrigues and J.P. Drummond: "Supersonic Combustion Experiment for CFD Model Development and validation", AIAA Paper No. 2004-266.

[10] P. G. Keislter, "A Variable Turbulent Prandtl and Schmidt Number Model Study for Scramjet Applications", Ph.D dissertation, Department of Mechanical and Aerospace Engineering, North Carolina State University, USA.

[11] Xiao, X., Edwards, J. R., Hassan, H. A., and Gaffney, R. L., "Role of Turbulent Prandtl Number on Heat Flux at Hypersonic Mach Numbers," AIAA Paper 2005-1098, 2005.

[12] Xiao, X., Hassan, H. A., and Baurle, R. A., "Modeling Scramjet Flows with Variable Turbulent Prandtl and Schmidt Numbers," AIAA Paper 2006-0128, 2006.

[13] Alexopoulos, G. A. and Hassan, H. A., "A k-ζ (Enstrophy) Compressible Turbulence Model for Mixing Layers and Wall Bounded Flows," AIAA Paper 1996-2039, 1996.

[14] Ingenito, A. and Bruno, C., "LES of a Supersonic Combustor with Variable Turbulent Prandtl and Schmidt Numbers," AIAA Paper 2008-0515, 2008.

[15] Ingenito, A. and Bruno, C., "Reaction Regime in Supersonic Flows," AIAA Paper 2009-0812, 2009.

[16] David M. Peterson, Graham V. Candler, and Travis W. Drayna "Detached Eddy Simulation of a generic scramjet inlet and combustor", AIAA Paper No. 2009-130.

[17] David M. Peterson, and Graham V. Candler: "Hybrid RANS/LES of a Supersonic Combustor". AIAA Paper No. 2008-6923.

[18] MSR Chandra Murty and Debasis Chakraborty: "Numerical Simulation of angular injection of Hydrogen fuel in scramjet combustor", ASME Journal of Aerospace Engineering (In press)

[19] Fluent 6.3 User's guide, 2006.

[20] Roe, P. L., "Characteristic based schemes for the Euler equations", Annual *Review of Fluid Mechanics*, 18:337–365, 1986.

[21] Magnussen, B. F., and Hjertager, B. H., "On Mathematical modeling of turbulent combustion with special emphasis on soot formation and combustion", *16th Symposium (International) on Combustion*, 1976, The Combustion Institute, Pittsburgh, pp. 719–729.

[22] I.R. Gran, M. C. Melaaen, and B.F. Magnussen: "Numerical simulation of local extinction effects in turbulent combustor flows of Methane and air" Twenty Fifth Symposium (international) on Combustion, 1994. pp 1283–1291.

[23] I.R. Gran, I.S. Erttesvag, B. F. Magnussen: "Influence of turbulence modeling on predictions of turbulent combustion ", AIAA Journal, Vol 35, No 1, pp 106–110, 1997.

[24] Yamashita, H., Shimada, M. and Takeno, T., " A numerical study of flame stability at transition point of diffusion flames", 26th Symposium (international) on combustion, The Combustion Institute. Pp 27–34.

[25] J.H. Kim, Y, Yoon, I S Jenng, Hwanil, Hug. J Y Choi, "Numerical study of mixing enhancement by shock where in model scramjet engine", AIAA J, Vol 41, No. 6, June 2003, pp 1074–1080.